


## Assessment of the origin and geothermal potential of the thermal waters by hydro-isotope geochemistry: Eskisehir province, Turkey

Galip Yuce, Francesco Italiano, Didem Yasin, Lutfi Taskiran & Ahmet Hilmi Gulbay


To cite this article: Galip Yuce, Francesco Italiano, Didem Yasin, Lutfi Taskiran & Ahmet Hilmi Gulbay (2017) Assessment of the origin and geothermal potential of the thermal waters by hydro-isotope geochemistry: Eskisehir province, Turkey, *Isotopes in Environmental and Health Studies*, 53:2, 198-211, DOI: [10.1080/10256016.2016.1206096](https://doi.org/10.1080/10256016.2016.1206096)

To link to this article: <http://dx.doi.org/10.1080/10256016.2016.1206096>

 View supplementary material 

 Published online: 13 Jul 2016.

 Submit your article to this journal 

 Article views: 135

 View related articles 

 View Crossmark data 



## Assessment of the origin and geothermal potential of the thermal waters by hydro-isotope geochemistry: Eskisehir province, Turkey

Galip Yuce<sup>a</sup>, Francesco Italiano<sup>b</sup>, Didem Yasin<sup>c</sup>, Lutfi Taskiran<sup>d</sup> and Ahmet Hilmi Gulbay<sup>c</sup>

<sup>a</sup>Department of Geological Engineering, Hacettepe University, Ankara, Turkey; <sup>b</sup>Istituto Nazionale di Geofisica e Vulcanologia, Sezione di Palermo, Italy; <sup>c</sup>Department of Geological Engineering, Eskisehir Osmangazi University, Eskisehir, Turkey; <sup>d</sup>General Directorate of Mineral Research and Exploration (MTA), Ankara, Turkey

### ABSTRACT

The thermal fluids vented over Eskisehir province have been investigated for their origin and to estimate the geothermal potential of the area. Thermal waters as well as bubbling and dissolved gases were collected and analysed for their chemical and isotopic features. Their isotopic composition varies in the range from  $-11.5$  to  $-7.7$  ‰ for  $\delta^{18}\text{O}$ ,  $-84$  and  $-57$  ‰ for  $\delta^2\text{H}$ , and  $0$ – $7.2$  TU for tritium. The gases (bubbling and dissolved) are mostly  $\text{N}_2$ -dominated with a significant amount of  $\text{CO}_2$ . The helium isotopic ratios are in the range of  $0.2$ – $0.66$  R/Rac, indicate remarkable mantle-He contribution ranging between  $2$  and  $10$  % in the whole study area. Considering the estimated geothermal gradient about three times higher than the normal gradient, and the reservoir temperatures estimated to be between  $50$  and  $100$  °C using quartz and chalcedony geothermometers, a circulation model was built where possible mixing with shallow waters cool down the uprising geothermal fluids.

### ARTICLE HISTORY

Received 18 February 2016  
Accepted 24 May 2016

### KEYWORDS

Carbon-13; carbon dioxide; Eskisehir; geothermal model; geothermometers; hydrogen-2; hydrogen-3; helium-3/helium-4; hydro-geochemistry; isotope hydrology; oxygen-18

## 1. Introduction

The increasing request for sustainable energy resources during the last decades pushed the scientists to improve their knowledge on geothermal systems and on the scientific approaches to constrain the natural systems and recover information on the feasibility of their exploitation.

The study area, marked by the diffuse presence of thermal waters, is located in central Anatolia near the North Anatolian Fault Zone. The area is crossed by active fault segments belonging to the Trace Eskisehir Fault Zone (Figure 1(a)) marked by active seismicity [1,2]. Results of earlier geophysical investigations [3–7] carried out over the region indicate the existence of buried tectonic structures in relation to hot water resources. Likewise, former investigations of the water geochemistry pointed out the relation of active tectonics with the potential geothermal reservoirs located in marble and schist levels as well as the water

**CONTACT** Galip Yuce ✉ [galipyuce@gmail.com](mailto:galipyuce@gmail.com) Department of Geological Engineering, Hacettepe University, Beytepe, Ankara, Turkey

Supplemental data for this article can be accessed at <http://dx.doi.org/10.1080/10256016.2016.1206096>.

© 2016 Informa UK Limited, trading as Taylor & Francis Group

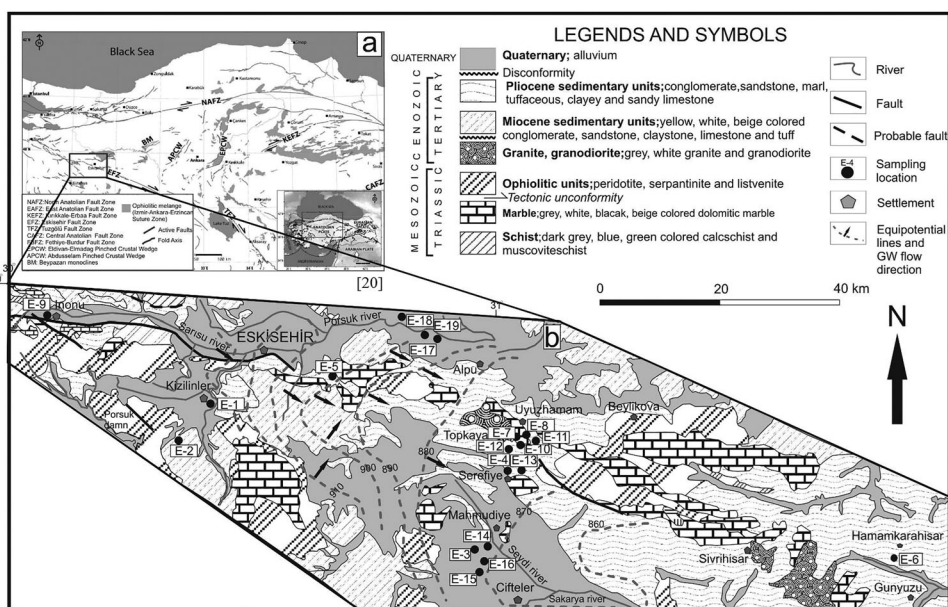


**Figure 1.** Geological map and locations of sampled waters in the area (modified after [13]) upper map from [20]).

radioactivity in the region [2,8–19]. As a matter of fact, there were enough evidences indicating the possibility that a consistent geothermal reservoir might be located in the Eskişehir area.

The relationships of the local geological and tectonic structures with the circulating fluids pose some limits on the location of the geothermal reservoirs and their thermal regimes. Many thermal springs and Turkish spas (Hammam), that are typical signs of deep fluids driven to the surface by fault activity, can be easily found in the central part of Eskişehir as well as in the close vicinity of the fault segments.

This paper accounts for assessments of the geochemical results related to 19 cold and hot water samples and 10 samples for gas analysis that allowed us to constrain the origin and gas/fluids interactions. Besides gas analysis, environmental isotope composition and R/Ra, He/Ne ratios as well as total  $\alpha$ ,  $\beta$ , and radon activity of the samples were examined.

## 2. Geologic and tectonic settings

Triassic metamorphic rocks and ophiolites represent the basement rocks in the region, which have been intruded by Palaeocene granitic rocks ([13]; Figure 1(b)). These are unconformably overlain by Miocene and Pliocene sediments, volcanic units, and Quaternary alluvium on top. The Lower Triassic metamorphic basement is composed of blue schist and marble, with a horizontal and vertical transitional contact. These metamorphic units are unconformably covered by ophiolitic rocks such as serpentinite, peridotite, and listwanite. The granodiorite cropping out in the Topkaya village is a product of magmatic activity developed as a result of crustal thickening during the Upper Cretaceous and Lower Eocene compressional tectonic regime. The Palaeocene age Topkaya granodiorite intruded the

basement rocks. Skarn zones were formed along the contacts with metamorphic rocks. All of the older units are unconformably overlain by the Middle–Upper Miocene sedimentary (a sequence of partly conglomerate, green claystone, coal, grey sandstone, dark grey to green siltstone, bituminous marl [21] and volcanic rocks, and Pliocene age sedimentary units). All these units are unconformably covered by Quaternary alluvium.

The Miocene and Pliocene sedimentary and volcanic rocks have been considered as cap rocks while the Palaeocene granites and metamorphic units (mainly schist and marble) act as reservoir for the thermal fluids. Because of the low permeability of the cap rocks, thermal waters cannot move upward unless connected by faults. Thus, faults in the area allow waters to infiltrate at depth where they warm up as a result of locally high geothermal gradient.

The imbricated structures are recorded resulting from evolving tectonic events during the closure of an ocean at the end of the Late Triassic period in the study area around Serefiye village (Eskisehir). The imbricated system that was evolved until the end of the Late Triassic was affected by later tectonic events [13]. During this period, N–S compression resulted in the evolution of E–W-trending fault systems. On the other hand, normal faults evolved under the effect of N–S extension along the Inonu–Eskisehir–Sivrihisar trend during the Neogene. These faults form a system, and they are observed at the south and north parts of Eskisehir. Synthetic and antithetic faults are evolved within this fault system.

A dextral strike-slip fault was observed along the granite–marble contact close to the study area around 10 km southeast (Kaymaz, north of Karakaya village). This fault is named as the Eskisehir fault zone [22] (Figure 1). The analysis of fault slip data shows a NW–SE compression and NE–SW extension in the region. Hot springs are located about 10 km southeast of the study area (Kaymaz, north of Karakaya village), and they are important manifestations of fault activity along this belt in the region. The possible western continuity of the dextral motion along the fault system and a small velocity difference in the western escape of the Anatolian block resulted in the development of the NW–SE-trending Late Pleistocene–Quaternary age Mahmudiye–Cifteler half graben.

Reservoir units are calc-schists and marbles within and around the studied area, while ophiolitic units and the Topkaya granodiorite have low permeability [23,24].

### 3. Materials and method

Two sampling campaigns were carried out in the wet and dry periods of 2006 and 2013. Four water samples were taken from wells (samples E3, E4, E5, and E8), four from cold groundwaters (E11, E12, E18, and E19), and from 11 thermal springs (samples E1, E2, E6, E7, E9, E10, E13, E14, E15, E16, and E17). A total of nine gas samples were collected (three bubbling and six dissolved gas samples) in 2013. The sampling locations are shown in Figure 1(b), while Table S1 (Supplemental Material [SM]) lists the types and locations of samples (given in UTM-WGS84 coordinates) along different segments of the Eskisehir Fault Zone.

Electrical conductivity (EC,  $\mu\text{S cm}^{-1}$ ), temperature ( $^{\circ}\text{C}$ ), pH, and redox potential (Eh, mV) values were measured *in situ* with a handheld multi-parameter instrument (YSI-556-USA brand). All samples were analysed for their major and minor ions, silica, B,  $\text{Br}^{-}$ , and  $\text{F}^{-}$  contents, environmental isotopes (oxygen-18, deuterium, tritium, and carbon-13), gas contents and noble gas isotope ratios as well as radioactivity parameters (radon, total alpha, and total beta). Chemical analyses were carried out using ICP-AES for Na, K, Ca,

and Mg, whereas  $\text{Cl}^-$ ,  $\text{SO}_4^{2-}$  and  $\text{HCO}_3^-$  concentrations were determined by titration method at the laboratories of the General Directorate of Mineral Research and Exploration (MTA), Ankara, Turkey. All samples are checked for the acceptable analytical error limits less than  $\pm 10\%$ , except for samples E5 and E12 (more than  $\pm 10\%$ ). Therefore, samples E5 and E12 were not considered for further evaluation, and they were disregarded. The isotopic ratios of  $^{18}\text{O}/^{16}\text{O}$  and  $^2\text{H}/\text{H}$  were determined by isotope-ratio mass spectrometry at the laboratories of the Technical Research and Quality Control Department of the State Hydraulic Works (DSI) in Ankara with an overall precision of  $\pm 1$  and  $\pm 0.1\%$  for  $\delta^2\text{H}$  and  $\delta^{18}\text{O}$ , respectively. The results are conventionally expressed in delta units as per mil deviation from the Vienna Standard Mean Ocean Water [25]. Tritium was analysed in the DSI laboratory with an ultra-low-level liquid scintillation counter (Perkin-Elmer Quantulus Ultra-Low-Level LSC) after electrolytic enrichment of the water samples with an error of  $\pm 0.6$  tritium units (TUs). The gross alpha and gross beta analyses were performed by Bertold Lb770-Pc 10-Channel Low-Level Alpha/Beta Counting System (TENNELEC LB 1000) in the DSI laboratory. The analytical errors in the gross alpha analyses (excluding Rn progenies) were min  $0.002\text{ Bq l}^{-1}$  and max  $0.056\text{ Bq l}^{-1}$ . The errors in gross beta analyses were min  $0.02\text{ Bq l}^{-1}$  and max  $0.15\text{ Bq l}^{-1}$ . The radon concentration was measured by GEO-RTM 2128 alpha spectroscopy (manufactured by SARAD GmbH). The relative statistical error for radon activities ranged from over  $10\%$  for low radon values ( $2\text{--}10\text{ Bq l}^{-1}$ ) to less than  $5\%$  for values greater than  $10\text{ Bq l}^{-1}$ . The measurement period was an hour with a high confidence level ( $95\%$ ) with respect to detection limits.

Samples for gas analyses were collected following already adopted methodologies for bubbling and dissolved gases [26,28]. The dissolved gases were extracted from water samples collected in 240 ml glass bottles sealed in the field by silicon/rubber septa using special pliers. All of the dissolved gas samples were collected taking care to avoid even tiny bubbles to prevent atmospheric contamination [26,27]. The free (bubbling) gases were collected using a stainless-steel inverse funnel connected to a three-way valve [29]. The valve was connected to a syringe and to a two-way Pyrex bottle with vacuum stop-cocks at both ends. The syringe sucked the gas collected by the funnel and through the valve; the gas was pushed inside the sampling bottle. The bottle was flushed with a gas amount ten times larger than its volume, and then the sample was collected following always the same procedure: the first valve is closed; the syringe applies a slight overpressure inside the bottle; and the second valve is finally closed.

The analysis of the bubbling gases was performed by direct injection in the gas chromatograph, while the dissolved gas analyses were carried out on the gas phase extracted after the attainment of the equilibrium (at constant temperature) between the water sample and a known volume of host, high purity gas (argon), injected inside the sampling bottle (see [26,27] for details). The chemical analyses of  $\text{He}$ ,  $\text{H}_2$ ,  $\text{O}_2$ ,  $\text{N}_2$ ,  $\text{CO}$ ,  $\text{CH}_4$ , and  $\text{CO}_2$  were carried out by a Perkin Elmer Clarus 500 gas chromatograph equipped with a double detector (TCD-FID; detection limits  $1\text{ ppm/vol}$ ), with argon as carrier gas.

The helium and carbon isotope analyses were carried out by mass spectrometry. Helium isotope analyses of both bubbling and dissolved gases (on gas fractions extracted following the same procedure as for the gas-chromatography and using nitrogen as host gas) were carried out after accurate sample purification following the already proposed procedures [26,28,30,31]. The isotopic analyses of the purified helium fractions were performed by a split flight tube static vacuum mass spectrometer (GVI5400TFT) that allows

the simultaneous detection of  $^3\text{He}$  and  $^4\text{He}$  ion beams, thereby keeping the  $^3\text{He}/^4\text{He}$  error of measurement to very low values. Typical uncertainties in the range of low  $^3\text{He}$  (radio-genic) samples are within  $\pm 1\%$ . The water samples for dissolved gas analyses were also used for the determination of the carbon isotopic ratio of the total dissolved inorganic carbon (TDIC). The method for  $\delta^{13}\text{C}_{\text{TDIC}}$  determination is based on the chemical and physical stripping of  $\text{CO}_2$ . The stripped gases, as well as the bubbling  $\text{CO}_2$ , were purified by means of standard procedures, then the carbon isotopic composition was measured using a Finnigan Delta Plus mass spectrometer, and the results are expressed in delta units as per mil deviation relative to the Vienna-Pee Dee-Belemnite standard. The standard deviation of  $\delta^{13}\text{C}$  is  $\pm 0.2\%$ .

#### 4. Results and discussion

The analytical results of waters and gases are listed in Tables S2 and S3 (SM), respectively. The results allowed us to group the groundwaters based on the major ion ratios, field parameters, dissolved gas contents, and saturation index (SI).

##### 4.1. Hydro-geochemical features

The dominant cations in waters are Mg in samples E-7 and E-19 (Figure 2(a)), and Na in samples E-1 and E-17 (Figure 2(b)), whereas Ca is the dominant cation for the rest of

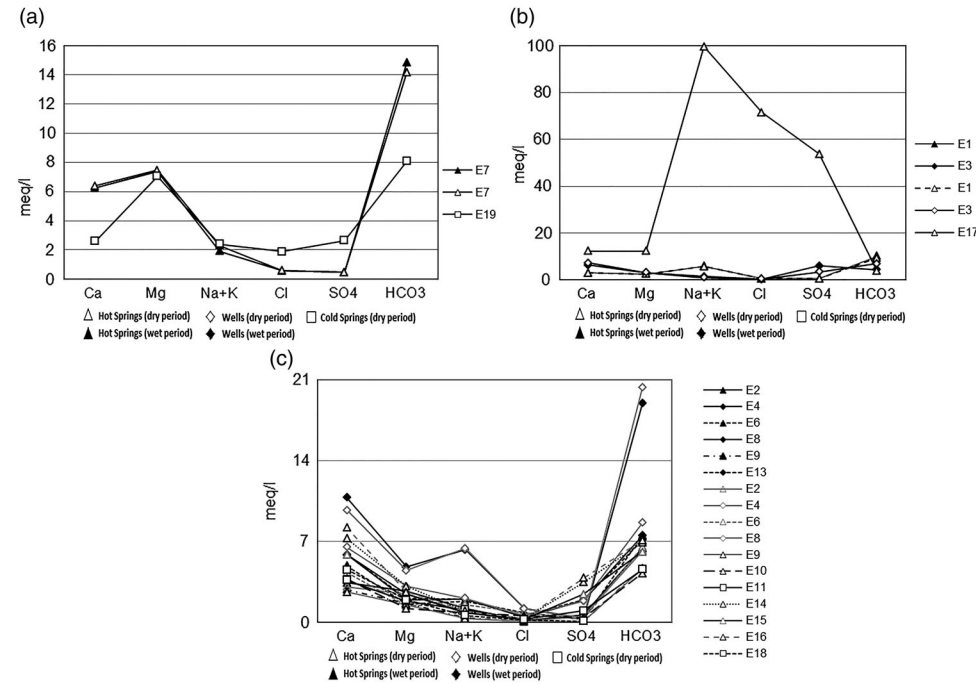


**Figure 2.** Semi-logarithmic Schoeller diagrams. They allow grouping of the collected samples as a function of the dominant hydrochemical facies. Three water types have been identified: (a)  $\text{Mg HCO}_3$ ; (b)  $\text{Ca Na Cl HCO}_3$  (except for E-17 and E-1 with  $\text{Na Cl HCO}_3$ , respectively); and (c)  $\text{Ca Na HCO}_3$  (mixed waters).



water samples (Figure 2(c)). The dominant anion is sulphate for sample E-3, chloride for sample E-17 (Figure 2(b)), and  $\text{HCO}_3$  for all other waters (Figure 2(c)) (Table S2).

The high Na and Cl contents of the water sample E17 (Agapinar thermal spring) probably originate from bituminous marl and claystone interbedded with coal layers of Miocene age [21]. The presence of a considerable amount of coal deposits and coal seams was recently discovered in the Neogene Basin of the Eskisehir Graben Area.

Hydrochemical characteristics of water samples do not show any seasonal change possibly indicating a long and deep groundwater circulation system unaffected by seasonal variations.

The Na  $\text{HCO}_3$  type water (sample E1) is the result of water–rock interactions (WRIs) with the calc-schists hosting reservoir, while Ca/Mg  $\text{HCO}_3$  type waters (Table S2) may have originated from marbles. However, the dominant presence of Mg and Na in some water samples is probably due to the interaction with the olivine and pyroxene minerals, as much as albite plagioclase in ophiolitic rocks [32] outcropping in the area, whereas sulphate may be resulted from oxidation of sulphide mineral such as pyrite in ophiolites or diffusion of sulphate from clays in overlying beds.

The saturation index (SI) values with respect to the minerals calcite and dolomite were calculated using the WATSPEC computer program [33]. The SI values calculated for common mineral dissolution are plotted in Figure S1(a,b) (SM) for dry and wet periods, respectively. They vary from  $-2.5$  to  $+1.75$  showing slight over-saturation with respect to both calcite and dolomite due to WRI occurrence with carbonate rocks. The results of SI calculations revealed that aragonite, calcite, chalcedony, dolomite, and quartz are over-saturated, indicating in all likelihood the dissolution of Triassic marble, which is considered the reservoir rock. As expected from the geological point of view, the waters are undersaturated to the respect of anhydrite and gypsum due to the absence of evaporites as a source rock. Sample E10 is oversaturated in aragonite, calcite, and quartz, probably from hydrothermal alteration of silica-enriched conglomerate, and undersaturated in anhydrite, chalcedony, dolomite, and gypsum. There are no seasonal variations regarding saturation minerals.

#### 4.2. Isotopes in water

According to deuterium and tritium values (Table S2), the sampled waters are considered as replenishment from relatively higher altitude (800–1000 m a.s.l.) and deep circulation due to the low  $\delta^2\text{H}$  (less than  $-75\text{‰}$ ) and low tritium (0–1.5 TU) values except for samples E18 and E19, which probably underwent evaporation process after sampling. Generally, seasonal effects can be identified on the samples relative enriched  $^{18}\text{O}$  and  $^2\text{H}$  in the dry period. E1 and E13 groundwater/thermal water samples marked by the most negative  $\delta^2\text{H}$  and  $\delta^{18}\text{O}$  values show typical altitude effect [34] implying the highest recharge areas among the collected samples (Figure 3).

#### 4.3. Chemistry and isotope signature of gases

The analytical results of nine samples taken from eight different sites are listed in Table S3 (SM). A common feature of both dissolved and bubbling gases is the large amount of  $\text{N}_2$  and low oxygen concentration indicating that nitrogen is only partially atmospheric.

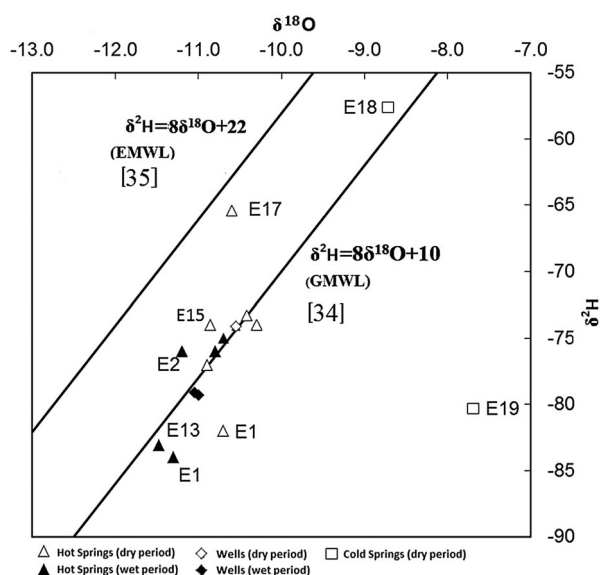


**Figure 3.**  $\delta^{18}\text{O}$ – $\delta^2\text{H}$  diagram. Almost all the samples fall on a line that can be considered as the local precipitation line. The line is parallel to the Eastern Mediterranean Meteoric Water Line due to the continental effect [35].

The triangular diagram of Figure 4 plots the relative amounts of  $\text{N}_2$ ,  $\text{CO}_2$ , and  $\text{CH}_4$ . The asterisk shows the  $\text{N}_2$  excess with respect to the atmosphere assuming that deep gas is oxygen-free. The  $\text{CO}_2$  content, ranging from 0.3 to >90 %, supports the presence of volatiles of deep provenance (either of crustal or mantle origin). Although a significant atmospheric content is expected for the dissolved gases, the high  $\text{CO}_2$  amount recorded in dissolved gas samples E1 and E4 (Table S3) confirms the interaction and dissolution of deep-originated volatiles to the local groundwater.

The  $\text{CH}_4$  and He contents provide additional information on the mixing of volatiles. At times,  $\text{CH}_4$  is present in significant amounts. As  $\text{CH}_4$  is usually generated from the crustal environment, and  $\text{CO}_2$  is either produced by crustal and mantle sources, we may discriminate the origin of the gaseous components using the isotopic ratio of helium.

The relationships between  $\text{CO}_2$  and  $\text{N}_2$  highlight also the occurrence of phenomena that change the pristine gas assemblage. Gas–water interactions (GWIs), namely the interactions occurring during gas uprising across the groundwater, allow the soluble species to dissolve and the less soluble gases to be enriched in the residual gas phase. Figure 5 shows that the  $\text{N}_2$  content decreases with increasing  $\text{CO}_2$  content, as  $\text{CO}_2$  dissolves in water, the less soluble  $\text{N}_2$  increases its concentration. Thus, the  $\text{CO}_2$ – $\text{N}_2$  relationship is a consequence of two different, sometimes concomitant phenomena: mixing of fluids from two different sources and GWIs leading to  $\text{CO}_2$  dissolution and virtual enrichment in the gas phase of the less soluble gas species. As a matter of fact, most of the bubbling gases are  $\text{CO}_2$ -dominated, whereas the dissolved gases are mainly composed of  $\text{N}_2$ .

The isotopic composition of helium is well known to be able to discriminate the genetic origin of helium and the associated volatiles. As stated above, large  $\text{CO}_2$  content testifies the presence of a gas phase of deep origin but cannot discriminate whether it was derived



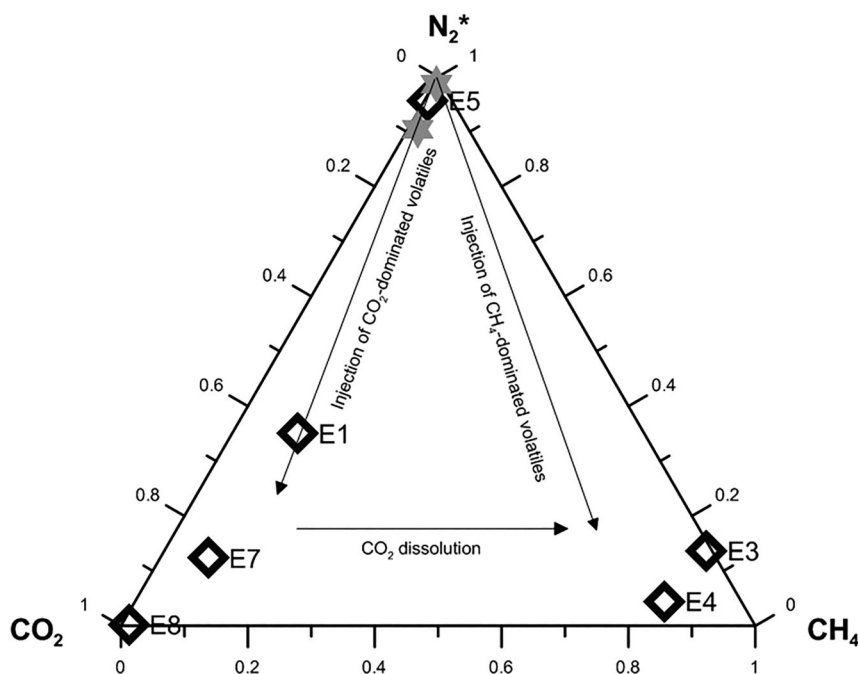


**Figure 4.** The triangular diagram shows the relative amounts of  $N_2$ ,  $CO_2$ , and  $CH_4$ . The asterisk shows the  $N_2$  excess to the respect to the atmosphere assuming that a deep gas is oxygen-free. To calculate: take the oxygen content and multiply by 2 for dissolved and by 3.7 for bubbling (2 and 3.7 are the  $N_2/O_2$  ratios in air and in air-saturated water). This is the amount of nitrogen related to the atmosphere, then subtract this amount to the total amount of nitrogen. The result is the nitrogen that does not come from the atmosphere.

from mantle or a mantle-derived source or from a crustal source. The values we recorded are in the range from 0.2 to 0.66 Rac, where Rac stands for isotopic ratios normalized to the atmosphere and corrected for the atmospheric contamination. We estimated the relative mixing proportion of helium from the three sources (air, mantle, and crust) as suggested by [36] assuming as mantle end-member the SCEM-type mantle (6.5 Ra [37]).

The C isotopic composition of  $CO_2$  of  $-2.5\text{‰}$  as  $\delta^{13}C$  in bubbling gases and  $-5.9$  and  $-6.8\text{‰}$  in dissolved  $CO_2$  (TDIC) (Table S3) shows relatively negative values. Considering the isotopic fractionation occurring during gas dissolution, the heavier isotope ( $^{13}C$ ) is preferentially lost as bicarbonate ion producing more negative  $\delta^{13}C$  values in dissolved  $CO_2$  due to the enrichment in light carbon. As a matter of fact, since our data underwent fractionation effects, the pristine gases should have displayed more positive values allowing to rule out a major contribution from organic source (typically in the range  $<-20\text{‰}$ ). Moreover, the relatively higher isotopic ratio of the bubbling gases compared to the typical isotopic composition assumed for mantle-derived  $CO_2$  ( $-6.5\text{‰}$ ) suggests an origin of  $CO_2$  from a mixture in variable proportions of mantle and crustal  $CO_2$  probably from decarbonation processes.

In the absence of volcanic structures, we argue that deep lithospheric faults are able to drive mantle-type volatiles towards the surface, as previously observed along the EAFZ [27].

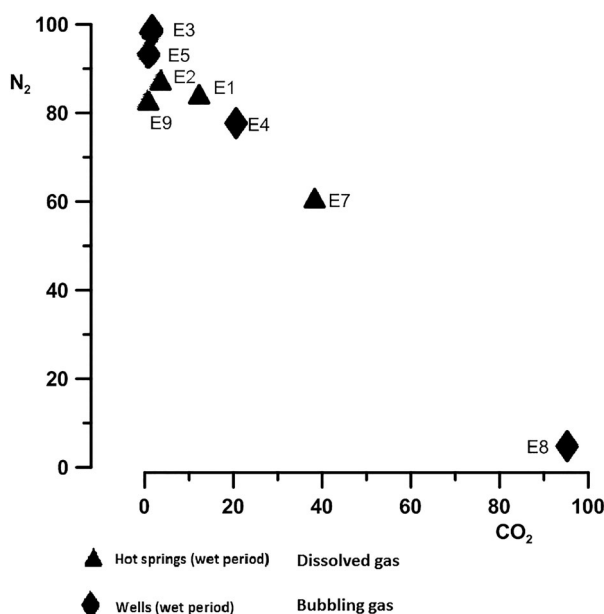


**Figure 5.** CO<sub>2</sub>–N<sub>2</sub> diagram. The relationships between the two gas species are the consequence of (1) mixing of two different gas assemblages and (2) GWI processes (dissolution).

#### 4.4. Silica geothermometers

The silica content of the water samples was investigated for its suitability as a geothermometer assuming that the temperature-dependent chemical reactions equilibrate in the aquifer and the equilibrium does not significantly change during fluids upraising. The quartz geothermometer has been tested for reservoir conditions >150 °C, as well as chalcedony geothermometer for temperatures <150 °C. Once the geothermometer indicates temperatures of 120–180 °C, then chalcedony may probably control the silica solubility. As the chalcedony geothermometer gives temperatures of 100–120 °C, it may represent a good estimation of the deep temperature [38]. The estimated reservoir temperatures of quartz and chalcedony geothermometers vary in the range from 80 to 120 °C and from 50 to 100 °C, respectively (Table S4), showing that they provide consistent results. The estimated temperatures of E10 and E17 are lower or close to the surface temperature either because of shallow circulation or possible silica precipitation during the ascent of the fluid to the surface. On the other hand, the presence of other salts enhanced the silica precipitation [39] as well (for the sample E17). Most of the pH values of the sampled waters are lower than 7.5 (Table S3) providing that the geotemperature estimations can be considered acceptable as no increase in dissolved silica content sourced from the low pH which might cause temperature overestimations [40–43].

#### 4.5. Circulation model

The interpretation of hydro-geochemistry and isotope geochemistry results allowed us to build up a circulation model and to identify the geo-tectonic conditions for a geothermal

reservoir, which is critical in assessing how to extract thermal waters. A possible geothermal model was developed taking into account the geological, hydrological, geochemical and hydrochemical data (Figure 6). The geological information identifies the calc-schists and marbles from metamorphic units as suitable reservoir rocks for geothermal waters with tectonically induced secondary porosity and permeability. The geochemical features of the circulating waters are consistent with equilibration of the thermal waters in marble host rocks. The major part of heat in the study area possibly originates from radioactive decay of U and Th in granitic rocks that outcropped in the study area [44] with contribution of mantle-derived volatiles [45]. The relatively higher total alpha vs total beta values are testified by the measured radon contents up to  $5600 \text{ Bq m}^{-3}$  (Table S2). In the absence of young volcanic rocks, only faults with lithospheric character are able to drive fluids from deep crustal levels. The faults are preferential way for water infiltration down to deep crustal levels where they warm up as a result of locally high geothermal gradient.

Based on the obtained data, two exploration wells were drilled (E4 and E3) in 2011, with the aim to gather direct information on the geothermal gradient. Following the well-logging in the Serefiye well (E4) at the depth of 665 m, the drilling stopped at the depth of 718 m due to sticking of the drilling pipes and also to protect the well from other risks. The measured temperature at the depth of 665 m was as  $65.7^\circ\text{C}$  after a time interval of 15 min. The yield of the well was determined as to be  $80 \text{ l s}^{-1}$  by pressure test. A geothermal gradient of the specific area can be calculated by following equation [46]:

$$\text{Geothermal gradient} = \frac{\text{measured BHT} - \text{mean annual surface temperature}}{\text{formation depth}}.$$

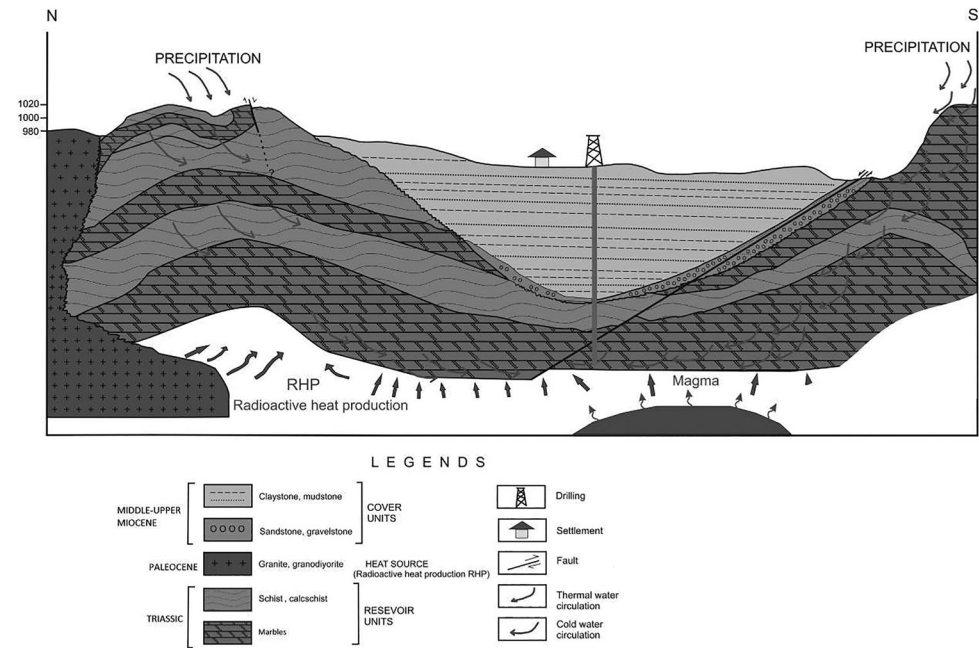


**Figure 6.** Geothermal model of the study area (vertical axis is not to scale).

Assuming a mean annual surface temperature of 11 °C (according to the Turkish Meteorological Service), the calculated geothermal gradient in the Serefiye well is 8.2°C/100 m. Another exploration well (Mahmudiye well E3) encountered the fault zone at 556 m where the drilling stopped due to circulation loss. The thermal water in the well was not in artesian conditions, temperature and flow rate measurements gave 59.5 °C and 70 l s<sup>-1</sup>, respectively, resulting in a geothermal gradient of 8.7 °C/100 m. Therefore, the water temperatures in well E3 increased at the reservoir level (located in marbles), in contrast to the water temperature in well E4 that constantly increased with the depth due to artesian flow condition. The direct observations provided reservoir temperatures lower by about 20 °C in respect of those estimated by the geothermometric approach thus apparently inconsistent. However, mixings with surface waters at shallow levels might cool down the geothermal fluids may provide an explanation for the observed results.

## 5. Conclusions

Results from a multidisciplinary study combining geology with hydro-geochemistry and isotope geochemistry carried out over the area of Eskisehir allowed us to constrain the existence and thermal potential of some aquifer systems. The geothermal resource is at the exploitable yield, and our results provide useful information on the natural progress controlling the geothermal regime. Based on the overall data evaluation, the most promising areas seem to be the located in the vicinity of Serefiye and Mahmudiye villages.

The heat source of the geothermal system for the eastern sector of the study area can be sourced from the radioactive decay of U and Th in the granite and granodiorite rocks; however, the isotopic ratio of helium in most of the samples is higher than crustal volatiles (0.02–0.05 Ra) indicating a significant mantle-He degassing over the whole study area probably due to the presence of lithospheric structures. The helium isotopic ratio points to a mantle and crustal sources mixing with an estimated mantle contribution in the range of 2–10 %.

Direct observations carried out during drilling of boreholes E3 and E4 have shown that the geothermal gradient in the area is higher than the normal one. According to the calcedony geothermometer, the reservoir temperatures of thermal waters were estimated between 50 and 100 °C.

Although the recorded temperatures are not high enough to produce electricity, the geothermal energy can be used to heat up residences and greenhouses, which is common in the region. It is worth to note that besides possible exploitation, it is mandatory to keep the equilibrium between the proportion of thermal water that can be exploited and the natural recharge of groundwaters. To keep the correct balance between the rate of water recharge and the required thermal energy to heat up the cold waters, an upper limit for the water pumping rate out of the reservoir has to be defined. For this reason, we suggest to fix the maximum productive yield in 50 l s<sup>-1</sup> for each geothermal well in the region. If the limit is overtaken, then an enhanced mixing with the shallow cold water component would cool down the reservoir in a short time.

Although a variety of scientific studies have significantly improved the knowledge on the natural resources of the area, no activity aimed to protect the Eskisehir–Mahmudiye–Cifteler and Alpu geothermal fields has been carried out. Some work needs to be

done to keep the geothermal fields safe and to prevent possible pollution for example because of new boreholes (already planned by MTA) and/or the development of new building complexes. The availability of a natural resource, like a geothermal reservoir, over long-time intervals requires in a mandatory way the protection from artificial modifications, biological/chemical contaminations, and mechanical effects.

## Acknowledgements

The authors thank the geochemical laboratories of INGV-Palermo (Italy) for the valuable analytical work.

## Disclosure statement

No potential conflict of interest was reported by the authors.

## Funding

This work has been supported by Hacettepe Üniversitesi [project no. FED-2015-5384] and General Directorate of Mineral Research and Exploration of Turkey (MTA).

## References

- [1] Yaltirak C, Yalcin T, Yuce G, et al. Water level changes in shallow wells before and after the 1999 Izmit and Düzce earthquakes and comparison with long-term water-level observations (1999–2004), NW Turkey. *Turk J Earth Sci.* **2005**;14:281–309.
- [2] Yuce G, Ugurluoglu YD, Nadar N, et al. Monitoring of earthquake precursors by multi-parameter stations in Eskisehir region (Turkey). *Appl Geochem.* **2010**;25:572–579.
- [3] Ozyazici E. [Resistivity and thermic survey of Eskisehir]. General Directorate of Mineral Research and Exploration Ankara Report No. 3230; **1962**. Turkish.
- [4] Erden F. [Gravity survey of Eskisehir–Mihalıcık region]. General Directorate of Mineral Research and Exploration Ankara Report No. 6290; **1971**. Turkish.
- [5] Gursoy T. [Detailed geothermal gravity survey of Eskisehir]. General Directorate of Mineral Research and Exploration Ankara Report No. 7725; **1975**. Turkish.
- [6] Mumcu N. [Geophysical survey of Eskisehir–Mahmudiye–Cifteler areas]. DSI Report No. 49. Eskisehir: State Hydraulic Works; **1976**. Turkish.
- [7] Demiroglu M. *Eskişehir–sivrihisar–günyüzü Havzası Hidrojeolojisi Ve Hidrojeokimyası [Hydrogeology and hydrogeochemistry of Eskisehir–Sivrihisar–Gunyuzu basin]* [PhD thesis]. Istanbul: Istanbul Technical University; **2009**. Turkish.
- [8] Erisen B. [Hydrogeological report of Hamamkarahisar–Sivrihisar thermal spring]. General Directorate of Mineral Research and Exploration Ankara Report No. 7088; **1974**. Turkish.
- [9] Kocak A. [Hydrogeological survey of Mihalıcık Yarıklı thermal spring]. General Directorate of Mineral Research and Exploration Ankara Report No. 5818; **1975**. Turkish.
- [10] Olmez E. [Geothermal potential of Eskisehir]. General Directorate of Mineral Research and Exploration Ankara Report No. 1985; 7798. Turkish.
- [11] Senturk N. [Conservation areas report of Eskisehir thermal water]. General Directorate of Mineral Research and Exploration Ankara Report No. 9231; **1991**. Turkish.
- [12] Goncuoglu MC, Dirik K, Erler A, et al. [Basic geological problems of Western Salt Lake (Tuz Golu) basin]. TPAO Report No. 3753. Ankara: Turkish Petroleum Cooperation; **1996**. Turkish.
- [13] Gozler MZ, Cevher F, Ergul E, et al. [Geology of middle and southern parts of Sakarya basin]. General Directorate of Mineral Research and Exploration Ankara Report No. 9231; **1997**. Turkish.

- [14] Guner F, Guner IN. Determination of hydrogeology of the karstic springs of Sakarbasi (Cifteler–Eskisehir) using hydrochemistry and environmental isotope techniques. Symposium of isotope techniques in hydrology; 2002; Adana. p. 207–212.
- [15] Selcuk AS, Gokten S. Neotectonical characteristics of the Inonu–Eskisehir fault system around Kaymaz (Eskisehir) region: influence on the development of the Mahmudiye–Cifteler half-graben Inonu. Active Tectonics Conference (ATAG). Ankara: Ankara University; 2004.
- [16] Sahin SY, Ozgun Y, Gungor Y. Geochemistry of U/TH enriched radioactive granitoids: Kestanbol and Kaymaz Plutons, Western Anatolia, Turkey. 57th Geological Congress of Turkey. Ankara; 2004. p. 48–49.
- [17] Demiroren M. [Resistivity survey of Eskisehir and its surrounding area]. General Directorate of Mineral Research and Exploration Ankara Report No. 6273; 1976. Turkish.
- [18] Demirbilek M, Mutlu H. Geochemical, geochronologic and Sr/Nd isotopic characteristics of the late Paleocene–middle Eocene granitoids in the Tavşanlı zone, NW Turkey. International Earth Science Colloquium on the Aegean Region (IESCA-2012). İzmir, Turkey; 2012.
- [19] Yuce G, Gasparon M. Preliminary risk assessment of radon in groundwater: a case study from Eskisehir, Turkey. Isot Environ Health Stud. 2013;49:163–179.
- [20] Seyitoglu G, Ecevitoglu B, Kaypak B, et al. Determining the main strand of the Eskişehir strike-slip fault zone using subsidiary structures and seismicity: a hypothesis tested by seismic reflection studies. Turk J Earth Sci. 2015;24:1–20.
- [21] Senguler I, Izlandi E. Neogene stratigraphy of the Eskisehir Graben and the investigation of coal deposition by seismic reflection method. Bull Mineral Res Explor. 2013;146:105–116.
- [22] Kocyigit A. Changing stress orientation in progressive intra-continental deformation as indicated by the neotectonics of the Ankara region (NW of Central Anatolia). Bull Turkish Petrol Geol. 1991;3:48–55.
- [23] Taskiran L. [Determination of geothermal energy potential Mahmudiye and Alpu Region (Eskisehir)] [PhD Thesis]. Eskisehir: Eskisehir Osmangazi University; 2014. Turkish.
- [24] Yuce G, Italiano F, Taskiran L, et al. Hydrogeochemical characteristics of low-enthalpy geothermal waters from Eskisehir province (Turkey). Proceedings World Geothermal Congress 2015; Melbourne, Australia.
- [25] Verhagen BT, Geyh MA, Froehlich K, et al. Isotope hydrological methods for the quantitative evaluation of groundwater resources in arid and semi-arid areas. Research Reports of the Federal Ministry for Economic Cooperation of the Federal Republic of Germany Bonn No. 7; 1991.
- [26] Italiano F, Bonfanti P, Ditta M, Petrini R, Slejko F. Helium and carbon isotopes in the dissolved gases of Friuli region (NE Italy): geochemical evidence of CO<sub>2</sub> production and degassing over a seismically active area. Chem Geol. 2009;266:76–85.
- [27] Italiano F, Sasmaz A, Yuce G, Okan OO. Thermal fluids along the East Anatolian Fault Zone (EAFZ): geochemical features and relationships with the tectonic setting. Chem Geol. 2013;339:103–114.
- [28] Italiano F, Yuce G, Uysal IT, Gasparon M, Morelli G. Insights into mantle-type volatiles contribution from the dissolved gases in artesian waters of the Great Artesian Basin, Australia. Chem Geol. 2014;378–379:75–88.
- [29] Yuce G, Taskiran L. Isotope and chemical compositions of thermal fluids at Tekman Geothermal Area (Eastern Turkey). Geochem J. 2013;47:423–435.
- [30] Sano Y, Wakita H. Precise measurement of helium isotopes in terrestrial gases. Bull Chem Soc Jpn. 1988;61:1153–1157.
- [31] Hilton DR. The helium and carbon isotope systematics of a continental geothermal system: results from monitoring studies at Long Valley caldera (California, U.S.A.). Chem Geol. 1996;127:269–295.
- [32] Dilek Y, Thy P. Island arc tholeiite to boninitic melt evolution of the Cretaceous Kizildag (Turkey) ophiolite: model for multi-stage early arc–forearc magmatism in Tethyan subduction factories. Lithos. 2009;113:68–87.
- [33] Wigley TML. WATSPEC: a computer program for determining the equilibrium speciation of aqueous solutions. British Geomorphology Research Group Technical Bulletin; 1977. p. 20–48.



- [34] Craig H. Isotopic variations of meteoric waters. *Science*. 1961;133:1702–1703.
- [35] Gat JR, Carmi L. Evolution of the isotopic composition of atmospheric waters in the Mediterranean Sea area. *J Geophys Res*. 1970;75:3039–3048.
- [36] Sano Y, Wakita H. Geographical distribution of  $^3\text{He}/^4\text{He}$  in Japan: implications for arc tectonics and incipient magmatism. *J Geophys Res*. 1985;90:8729–8741.
- [37] Dunai TJ, Baur H. Helium, neon and argon systematics of the European subcontinental mantle: implications for its geochemical evolution. *Geochim Cosmochim Acta*. 1995;59:2767–2783.
- [38] Karingithi CW. Chemical geothermometers for geothermal exploration. Presented at Short Course IV on Exploration for Geothermal Resources organized by UNU-GTP KenGen and GDC Kenya; 2009. p. 1–22.
- [39] Andhika M, Castaneda MH, Regenspurg S. Characterization of silica precipitation at geothermal conditions. *Proceedings World Geothermal Congress 2015, Melbourne, Australia*; 2015. p. 19–25.
- [40] Gulec N. Applications of geothermometry. In: Savaşçın MY, Mertoğlu O, editors. *Geothermal geochemistry and some new geothermal approaches. Reviewed Course Book of International Summer School on Geothermal Geochemistry İzmir*. İzmir: The publications of Dokuz Eylül University; 2005. p. 85–103.
- [41] Fournier RO. Chemical geothermometers and mixing models for geothermal systems. *Geothermics*. 1977;5:41–50.
- [42] Arnorsson S, Gunnlaugsson EH, Svavarsson H. The chemistry of geothermal waters in Iceland. III. Chemical geothermometry in geothermal investigations. *Geochim Cosmochim Acta*. 1983;47:567–577.
- [43] Fournier RO. Chemical geothermometer and mixing models for geothermal systems. *Geothermics*. 1977;5:41–50.
- [44] Orgun Y, Altınsoy N, Gültekin AH, Karahan G, Çelebi N. Natural radioactivity levels in granitic plutons and groundwaters in Southeast part of Eskisehir Turkey. *Appl Radiat Isot*. 2005;63:267–275.
- [45] Torgersen T, Habermehl MA, Clarke WB. Crustal helium fluxes and heat flow in the Great Artesian Basin Australia. *Chem Geol*. 1992;102:139–152.
- [46] Forrest J, Marcucci E, Scott P. Geothermal gradients and subsurface temperatures in the northern Gulf of Mexico. *Trans GCAGS*. 2005;55:233–248.